COMITATO NAZIONALE PER L'ENERGIA NUCLEARE
Laboratori Nazionali di Frascati

LNF-76/33(R)
8 Giugno 1976

R. Bartiromo, E. Borsella, F. Campolungo and S. Mobilio :

MAGNETO-OPTICAL SPECTROSCOPY IN SOLIDS BY MAGNETIC FIELD MODULATION. I: EXPERIMENTAL TECHNIQUE AND ITS APPLICATION TO REFLECTANCE OF CdS.

Servizio Documentazione
dei Laboratori Nazionali di Frascati del CNEN
Casella Postale 70 - Frascati (Roma)

Laboratori Nazionali di Frascati
Servizio Documentazione

LNF-76/33(R)
8 Giugno 1976

R. Bartiromo[x], E. Borsella[x], F. Campolungo and S. Mobilio[x]:
MAGNETO-OPTICAL SPECTROSCOPY IN SOLIDS BY MAGNETIC FIELD MODULATION. I: EXPERIMENTAL TECHNIQUE AND ITS APPLICATION TO REFLECTANCE SPECTRA OF CdS.

1. - INTRODUCTION. -

The optical spectroscopy of solids began to be developed only in the 1950's, even if it was fundamental for the investigation of the band structure of solids. This was due to the difficulty of observing the broad optical structures of solids and to the lack of a theoretical support for the understanding of the experimental data. As a matter of fact, atomic and molecular spectroscopy had been widely studied since the absorption is resonant and easily connected to the energy difference between electronic states. On the other hand, in solid state spectroscopy the absorption does not show resonances since there are many electronic states separated by nearly the same energy difference and located in different points of the first Brillouin zone. In consequence of the theories developed since 1950's[1, 2, 3] it is nowadays well known that the absorption coefficient is given by[4]:

$$a = \frac{\varepsilon_2(\omega)\omega}{n(\omega)c} = \frac{\omega}{n(\omega)c}\left(\frac{8\pi^2 e^2}{m^2\omega^2}\right) \sum_{cv} \int_{B.Z.} \frac{d^3k}{8\pi^3} \cdot \left| M_{cv}(\underline{k}) \right|^2 \delta(E_{cv}(\underline{k}) - \hbar\omega) \qquad (1)$$

(x) - Istituto di Fisica Sperimentale dell'Università, Napoli.

with:

$$\left| M_{cv}(\underline{k}) \right|^2 = \left| \langle \psi_c(\underline{k}) | \underline{\varepsilon} \cdot \underline{p} | \psi_v(\underline{k}) \rangle \right|^2 ;$$

$\underline{\varepsilon}$ = Unit vector in the direction of the electric field;

$\underline{p}$ = Momentum operator;

$E_{cv}(\underline{k}) = E_c(\underline{k}) - E_v(\underline{k})$;

$E_c(\underline{k})$ = energy of conduction band;

$E_v(\underline{k})$ = energy of valence band;

$\hbar\omega$ = photon energy.

In (1) the integral is extended over the first Brillouin zone and the sum is over all the possible valence and conduction bands.

Since $\left| M_{cv}(k) \right|^2$ is nearly constant, it is the quantity

$$J_{cv}(\omega) = \frac{1}{(2\pi)^3} \int_{B.Z.} \delta(E_{cv}(\underline{k}) - h\omega)\, d^3\underline{k}$$

that contains all the informations on band structure achievable from the experimental knowledge of $\alpha(\omega)$.

The quantity $J_{cv}(\omega)$, called the joint density of states, is slowly varying in K-space except around the frequencies corresponding to the critical points K_c defined by the relation $\nabla_{\underline{k}} E_c(\underline{k}) = \nabla_{\underline{k}} E_v(\underline{k})$. On account of the remark that the structures in optical spectra are due to critical points, it has become possible to relate optical experiments to band structure calculations.

Unfortunately, the broad structures to be detected are usually superimposed on a structureless background, so that an instability of the order of 1% in the experimental apparatus is sufficient for hiding them. An extraordinary impulse to optical spectroscopy was given by the work of Seraphin[5] on modulated electroreflectance in Germanium; indeed, it is possible to obtain an improvement of two or three orders of magnitude in the sensitivity over conventional d. c. measurements if it is measured the derivative of the optical constants with respect to some external parameter (e. g. an electric field, a stress, etc.).

This may be accomplished by applying[5] a small periodic perturbation to the sample which gives rise to a modulation of the optical constants proportional to the derivative of the reflectance R.

The derivative signal is detected by means of phase sensitive analysis.

The main advantages of modulation techniques are[6]:

- a high sensitivity: percentual variations in the optical constants of the order of 10^{-6} are detectable;
- the optical structures are sharpened;
- the structures of the light source and the background are eliminated.

A remarkable progress has been accomplished by means of differential techniques also in magneto-optical spectroscopy[7]. The introduction of a magnetic field in optical measurements is extremely[6] important since it allows obtaining additional and original informations on the electronic properties of solids. Indeed optical spectroscopy allows determining only the location of the band edges on an energy scale, but little can be known about the band curvature, symmetries and locations within the Brillouin zone.

In the presence of a magnetic field H the absorption coefficient becomes[4]:

$$\alpha = \frac{4\pi c^2}{cn(\omega)m^2\omega} \left| M_{cv} \right|^2 \sum_{nk_yk_z} \delta\left(Eg + \left(N + \frac{1}{2}\right)\hbar\omega_\mu + \frac{\hbar k_z^2}{2\mu} - \hbar\omega\right), \tag{2}$$

with:

Eg = energy gap;

$$\omega_\mu = \frac{eH}{\mu c}\ ; \qquad \mu = \frac{m_c m_v}{m_c - m_v}\ ;$$

m_c = effective mass of conduction band;

m_v = effective mass of valence band.

In such a case, $J_{cv}(\omega)$ is proportional to the summation in formula (2); the plot of $J_{cv}(\omega)$ as a function of $(\hbar\omega - Eg)/\hbar\omega_\mu$ is reported in Fig. 1.

Since electronic transitions from the valence to conduction band take place with a probability proportional to $J_{cv}(\omega)$, it results evident from Fig. 1 that the presence of a magnetic field leads again to a resonance spectroscopy analogous to that carried out for atoms.

The distance between two consecutive peaks shown in Fig. 1 allows determining the effective masses and g factors; furthermore in a magnetic field the symmetry of the bands is lowered so that

some degeneracy is removed and new informations can be obtained on the location of band edges in K-space.

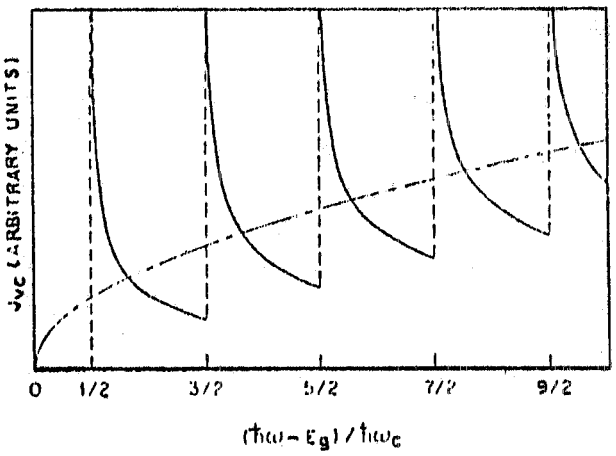

FIG. 1 - Joint density of states at a critical point Mo with isotropic effective mass tensor in the presence of a magnetic field. The zero field case is also shown (broken line).

Several differential techniques have been used successfully in the presence of a steady magnetic field[7]; to our knowledge, however, only one pioneering work[2] concerning the modulation of the magnetic field is reported in literature.

In this paper we describe an apparatus for the study of magneto-optical properties of solids by modulating the magnetic field and we report the experimental data on CdS.

We have prefered this kind of modulation since it presents at least the following advantages over the internal differential techniques :

a) The periodical perturbation is applied externally to the sample, therefore there are not restrictive requirements on the sample dimensions and mounting techniques ;
b) Magneto-optical structures are modulated directly and not via their dependence on other parameters such as temperature, electric field, etc. ; thus the theoretical analysis of the experimental data is not complicated by the effects due to the modulation parameter ;
c) High N quantum number Landau transitions are enhanced since the percentual variation of the absorption coefficient given by[7]:

$$\frac{\Delta\alpha}{\alpha} = \frac{1}{\alpha}\left\{\frac{C\omega_\mu}{2n(\omega)c\omega}\sum_N\left[\frac{(\omega-\omega_N)^{-1/2}}{H} + (N+\frac{1}{2})\omega_\mu \cdot \right.\right. \tag{3}$$

$$\left.\left. \cdot \frac{\partial}{\partial\omega_N}(\omega-\omega_N)^{-1/2}\right]\right\},$$

with :

$$\hbar\omega_N = Eg + (N + \frac{1}{2})\hbar\omega_\mu \; ; \qquad C = \left[2c^2(2\mu)^{\frac{3}{2}}/m^2\hbar^{\frac{5}{2}}\right]\left|M_{cv}\right|^2$$

is proportional to the N quantum number. This is a remarkable advantage since the spectral peaks become progressively weaker and broader with increasing N.

d) There is no restriction on the optical spectral range : this technique can be applied from the far infrared to the vacuum ultraviolet region. In the latter spectral region, very stimulating nowadays for the availability of synchrotron radiation sources, magneto-modulation might be very useful for studying new magneto-optical effects.

With regard to a comparison with external modulations[6], we remark that also these techniques offer the advantages a) and b). Unfortunately, if any external modulation is used, also the optical response of the whole optical system is modulated and this may give rise to a signal comparable or even larger than the one from the sample.

2. - DESIGN AND EXPERIMENTAL. -

Our apparatus has been designed for experiments at liquid helium temperature in a static magnetic field up to 60 Kgauss, produced by a superconducting solenoid.

The main technical problem we have had to overcome was the requirement of working with a modulation field ΔH (≤ 1 Kgauss) at a frequency high enough to avoid a large part of the low frequency noise and low enough to reduce liquid helium dissipation.

2.1. - Design procedure of the experimental apparatus.

The modulating field might be generated by a small a.c. current flowing through the superconducting solenoid[2].

Unfortunately, this simple solution has unavoidable experimental disadvantages. The inductance of the solenoid is so large that it is necessary to work at low frequency ($\simeq 10$ hertz) to obtain appreciable signals. But the widespread modulating magnetic field produces mechanical vibrations in the metallic dewar giving rise to a spurious signal in phase with the perturbation. This results in hiding completely the signal to be detected from the specimen.

To solve this problem we have designed the cryogenic part of our apparatus so that a small modulation coil may be put inside the superconducting solenoid. In consequence of these remarks the cryo

stat, Fig. 2, consists of:

a) a dewar containing the superconducting magnet;
b) a second dewar where sample and the modulation coil are cooled;
c) a "modulation" section, containing the coil and the sample holder, mounted in the second dewar.

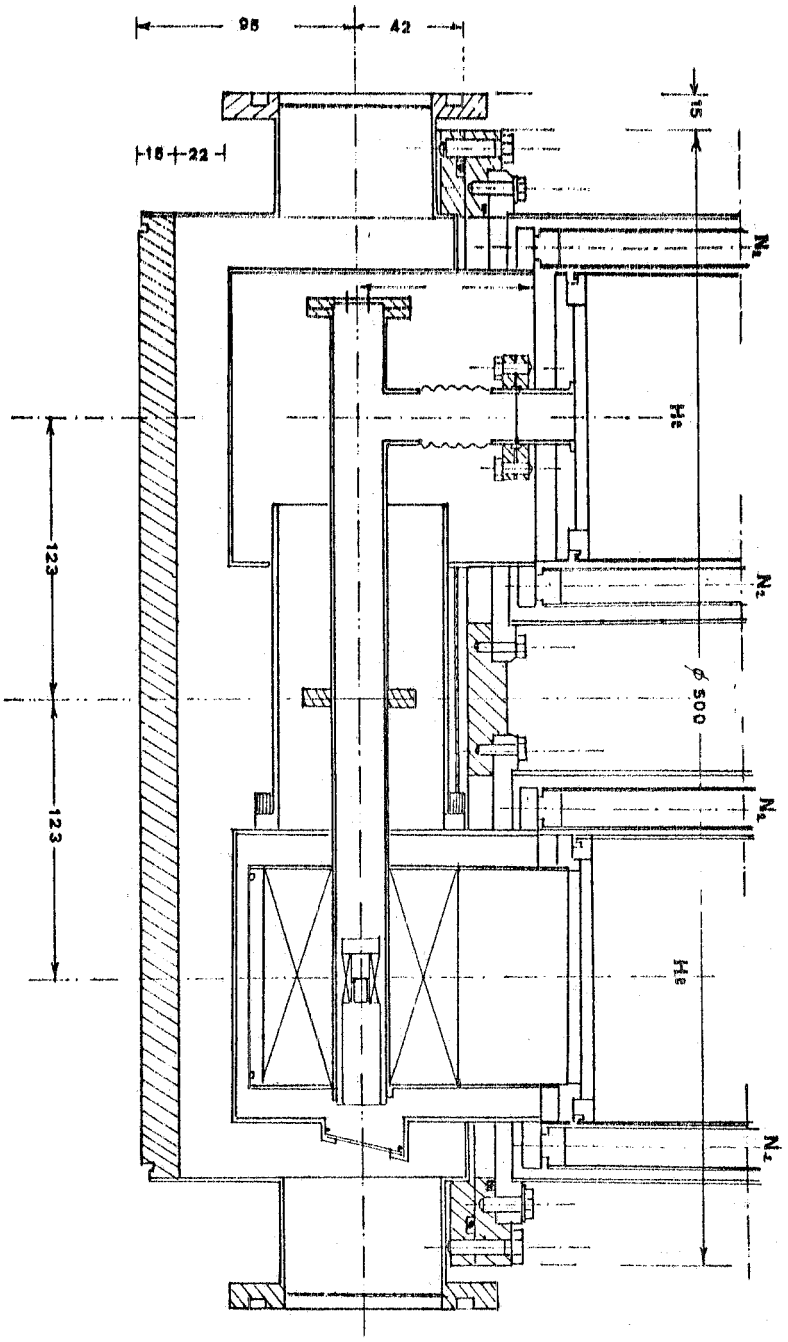

FIG. 2 - Cryogenic part of the experimental apparatus (the lenghts are in mm).

The copper wire coil is wounded on an insulating support to reduce the Foucault losses, and is immersed in liquid helium to minimize Joule dissipation. The coil is put at the center of the superconducting solenoid and is anchored to it in order to avoid mechanical vibrations caused by the oscillating magnetic field. The coil support is a PVC cylinder anchored by a 5 mils mylar ring to a stainless steel tube. The mylar ring is glued to the tube and to the PVC cylinder with an epoxy resin(x). The elasticity of mylar compensates the difference in thermal expansion between steel and PVC. The tube is soft-soldered to an external steel tubing as shown in detail in Fig. 3.

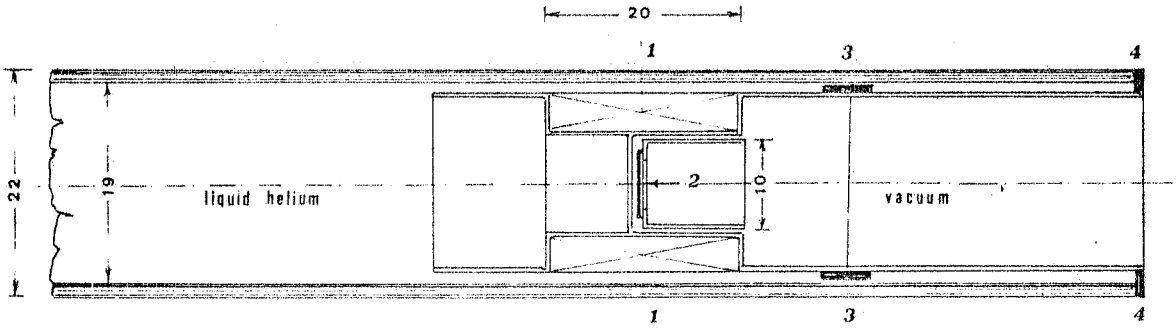

FIG. 3 - Details of the mounting of the coil support (the lenghts are in mm). 1 - coil; 2 - sample; 3 - mylar matching; 4 - soft soldering. The figures of the coil are the following: number of turns: 600; wire diameter: 0.35 mm; the resistance at 4.2°K is 0.3 ohm.

Liquid helium, flowing through these tubes, cools directly the coil and its support.

The sample is mounted on an insulating holder put at the common center of the coil and of the superconducting magnet; we have not immersed it in 4.2°K liquid helium to avoid the scattering of incident light by bubbling helium. This part of the apparatus for cooling the sample is shown in Fig. 3.

Thermal contact between the support of the coil and the holder of the specimen is guaranteed by a high thermal conductivity grease.

2.2. - The coil.

The design procedure of the coil is based essentially on the re

(x) - Epon resin 815 manufactured by Miller Stephenson Chemical Co. Inc. (50% b.w.) and epon V40 curring agent manufactured by Shell (50% b.w.).

quirement of minimizing Joule losses.

The power dissipation is given by:

$$p \simeq \frac{4\rho H^2}{f^2(\alpha,\beta)} \left(\frac{2}{\alpha - 1} + 1\right) L \ , \qquad (4)$$

where:

$\alpha = \frac{d + a}{d}$; $\beta = \frac{L}{2d}$ (see Fig. 4 for the meaning of d, a and L),

$$f(\alpha,\beta)^{(9)} = \beta \frac{\ln\left\{\left[\alpha + (\alpha^2 + \beta^2)^{1/2}\right] / \left[1 + (1 + \beta^2)^{1/2}\right]\right\}}{\alpha - 1} \ ,$$

$$H = \frac{nI}{L} f(\alpha,\beta) \ ,$$

with:

$$n \simeq \frac{La}{4r^2} \ ; \qquad l \simeq \pi n(d + a) \ ; \qquad R = \rho \frac{l}{\pi r^2}$$

S, R and 2n are respectively the resistivity, the resistance, the length and the diameter of the wire of the coil. In the previous formulas the length are expressed in cm; the current I in ampere and the magnetic field H in gauss.

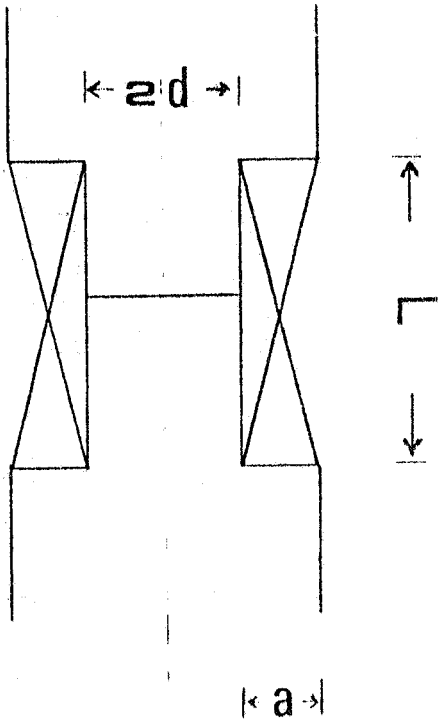

FIG. 4 - Parameters of the coil.

As shown in (4), thermal dissipation does not depend on wire size and is minimized when α is maximum and L is minimum. Restrictions on the maximum value of α are imposed by the limited space at our disposal, the minimum internal diameter of the coil is fixed by the size of the sample, while the maximum external diameter is determined by the size of the internal bore of the magnet. Finally the requirements on field homogeneity in the central region of the coil determine the minimum value of L. As a matter of fact the requirements on field

homogeneity are not too restrictive in our experiments, since the magnetic field generated by the coil is used only as a modulation parameter. The coil figures, so determined, are given in Fig. 3.

A 300 gauss effective magnetic field is generated by a 0.7 ampere a.c. current. Axial field inhomogeneity along two millimeters is less than 1%, while radial inhomogeneity along the entire diameter of the coil is less than 5%. Heat dissipation is caused by Foucault currents and by Joule losses, the former is proportional to the square of the frequency of the current and is strongly reduced by lowering the frequency, the latter is unavoidable and its value amounts to about 160 mW.

We have verified that at our working frequency (~170 hertz) the experimental helium evaporation rate is consistent with the above calculated value of Joule dissipation, and it does not vary appreciably by reducing the frequency to one half. In such conditions liquid helium wholly evaporates within 7 - 8 hours from our two dewars.

3. - EXPERIMENTAL DETAILS. -

In the following we describe the block scheme, Fig. 5, of the apparatus we are using for measurements of magneto-reflectance of CdS and CdSe by magnetic field modulation[10].

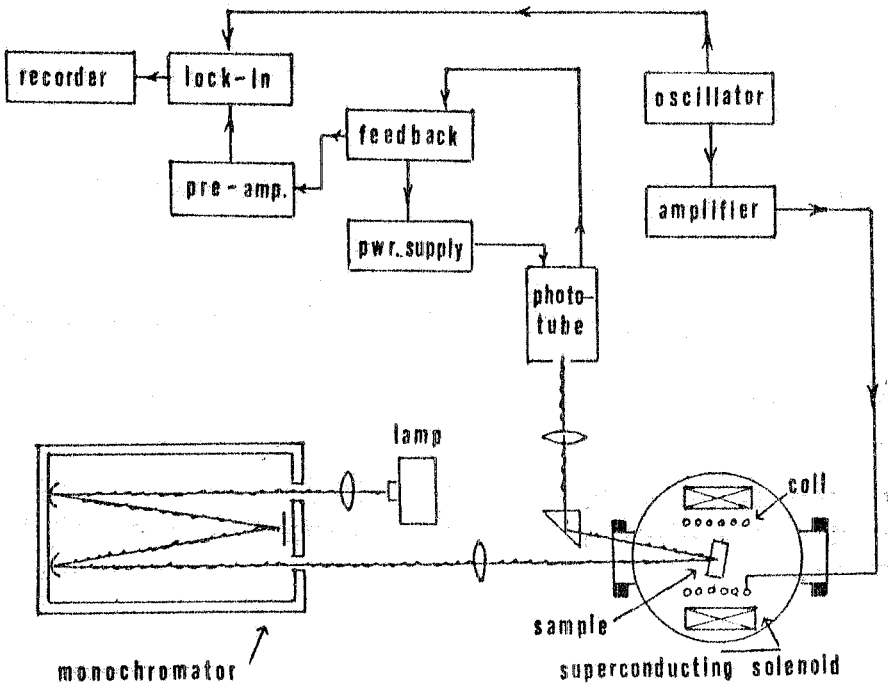

FIG. 5 - Block scheme of the actual apparatus.

The cryogenic part of our apparatus is shown in Fig. 2; both dewars are model MD4A dewars from Oxford Instruments, an Oxford superconducting solenoid provides magnetic fields up to 60 Kgauss with currents up to 60 amperes supplied by a Regatron current generator.

The light of a 150 watt XB0 Osram lamp can be monochromatized by a 1 m Jarrel-Ash Czerny-Turner spectrometer equipped with a 100×100 mm^2 1200 line/mm grating blazed at 3500 Å.

The light incident on the specimen is linearly polarized by a Thomson prism.

The reflected light is detected by an Emi 9558R photomultiplier (S-20 response), magnetically shielded.

By keeping the average photocurrent fixed (i. e. by normalizing the d. c. component of the light intensity) the modulated signal turns out to be indipendent of the incident intensity and proportional to $\Delta R/R$[6].

The voltage signal, in phase with the modulated magnetic field, is detected by a PAR 124 lock-in amplifier; the current is supplied to the modulation coil by a low frequency amplifier driven by the lock-in oscillator.

Continuos wavelenght scans are recorded on a strip-chart recorder; wave-lenght markers oan be used every 10 Å; wavelenght calibration is obtained by a low-pressure gas 1 amp.

4. - RESULTS ON CdS. -

With this apparatus, measurements have been executed on samples of wurzite type CdS.

Spectra have been recorded in Faraday configurations with the hexagonal axis of the crystal (C-axis) perpendicular to the field (the crystals have a reflecting surface of growth containing the C-axis). With an integration constant of 10 seconds, the signal to noise ratio was better than 10.

The crystals being uniaxial, the experiments were performed with linearly polarized light and we have analyzed the results in two configurations.

4.1. - E⊥C-axis.

Typical spectra for the n = 1 excitons ($\gamma_1 \approx 0.015$)(x) with the identifications of the observed structures, are shown in Fig. 6. It

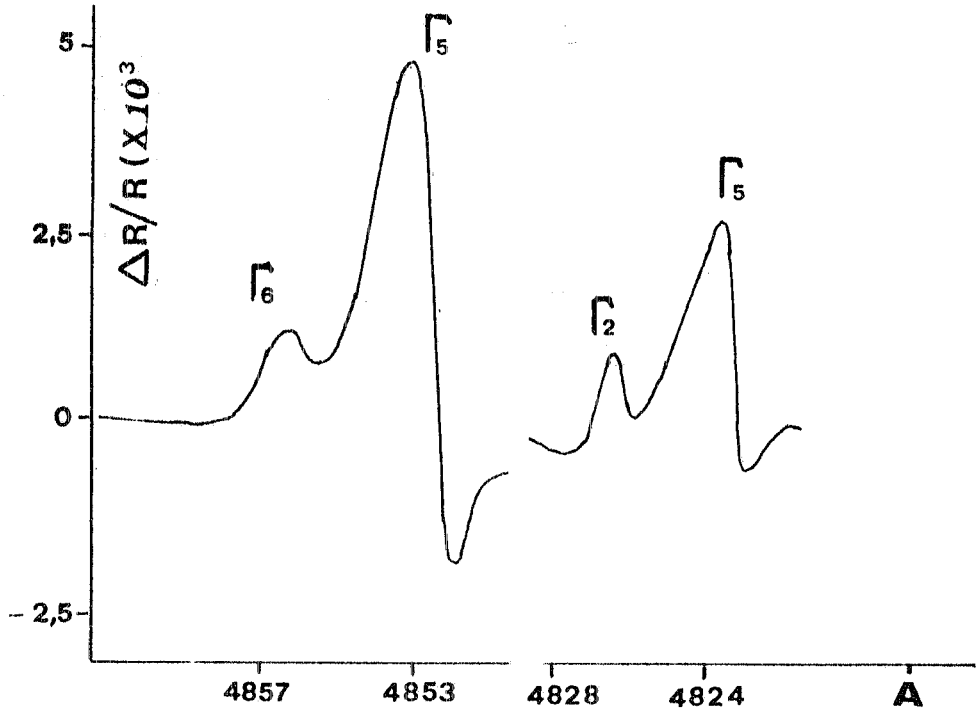

FIG. 6 - The N = 1 excitons of A and B edges in CdS (H = 50 Kgauss).

can be noticed that n = 1 excitonic level of the A edge is splitted into two components of Γ_5 (dipole allowed) and Γ_6 (dipole forbidden) symmetry[11, 12]. Since these states are mixed by a magnetic field perpendicular to the C-axis (Γ_5-type perturbation), both eigenstates have a Γ_5 component and become dipole allowed. These states are shown in Fig. 6; their identification is based on the line splitting and on the magnetic field dependence of the line intensities.

A similar analysis has been done for the n = 1 excitonic level of the B edge. This state is splitted into three components of Γ_1, Γ_2, and Γ_5 symmetry, the latter state being the only one dipole allowed. A group theoretical analysis shows that in Faraday geometry only the Γ_2 forbidden exciton becomes allowed. This explains the evidence for two transitions in the presence of the magnetic field as shown in Fig. 6. The Γ_2 exciton, which had not been previously ob

(x) - γ is the ratio between $\hbar\omega_\mu$ and the binding energy of the excitonic state[14].

served, is separated from the Γ_5 exciton by 1.4 meV.

Higher energy structures are shown in Fig. 7. They are interpreted as n = 2 excitonic transitions in the presence of a magnetic field and as transitions to N = 1 ($N_v = 1$, $N_c = 1$) and N = 2 ($N_v = 2$, $N_c = 2$) Landau levels of the conduction band modified by the coulombic interaction for both A and B edges. The positions of the latter lines agree with those of Shah[13].

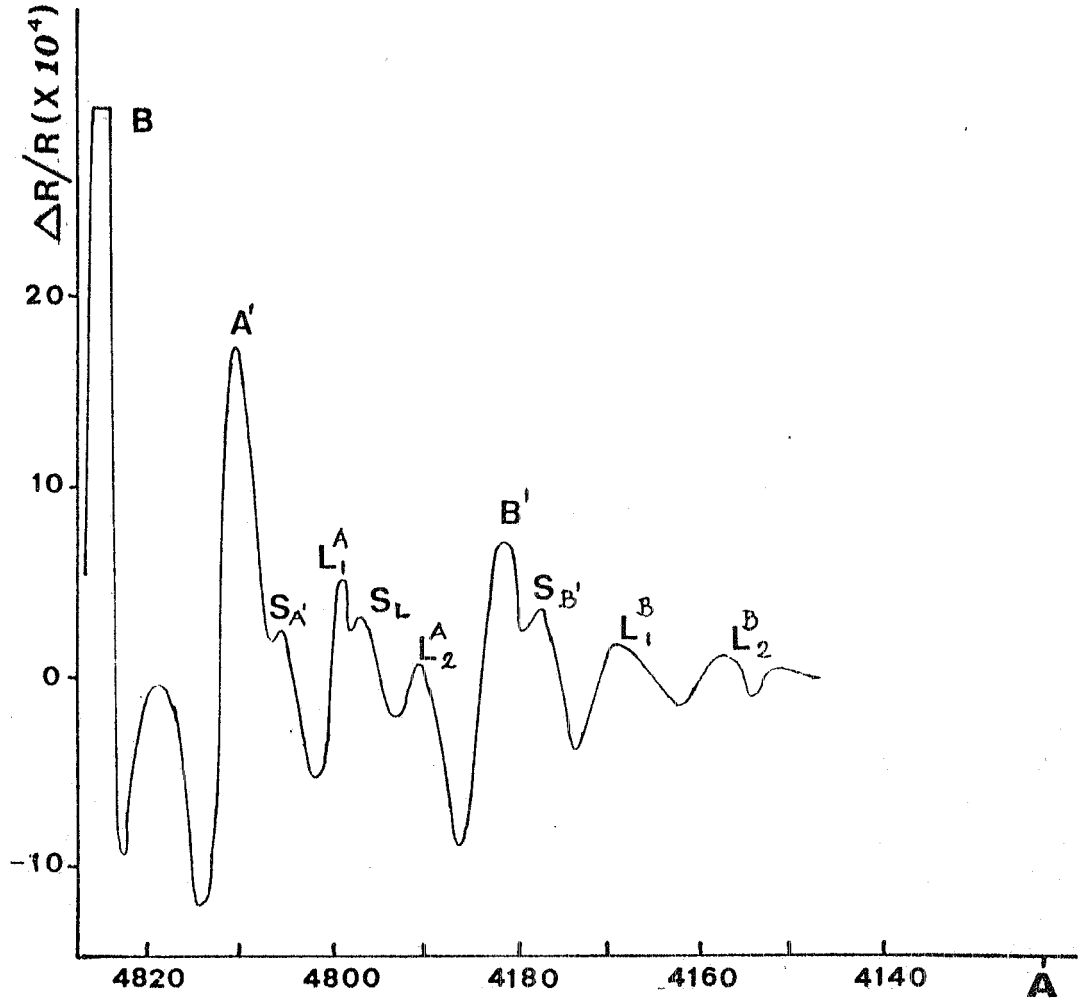

FIG. 7 - Landau transitions in CdS (H = 50 Kgauss, T = 10°K).

All above structures are splitted into two components, the higher energy one being denoted by S in Fig. 6. We attribute the existence of such components to the anisotropy of CdS and to the fact that the magnetic field is perpendicular to the C-axis. In this case the selection rule allows for transitions between Landau levels N = = 0, 2, 4, etc., and for excitonic transitions $m \neq 0$. We cannot make a detailed analysis of the n = 2 lines because $\gamma_2 = 0.2$ is too large for perturbation theory and too small for the adiabatic approxima-

tion[14]. For the Landau level transitions (L_1^A and L_2^A) a quantitative analysis can be performed in the adiabatic limit. The energies of the transitions are given by[15]:

$$E_{N_1\Delta N} = E_g(0) + (N + \tfrac{1}{2})\hbar\omega_\mu + N\hbar\omega_v \qquad (5)$$

with :

$$N = N_c \; ; \quad \Delta N = N_v - N_c \; ; \quad \omega_\mu = \frac{eH}{\mu} \; ;$$

$$\frac{1}{\mu} = \frac{1}{m_e} + \frac{1}{\sqrt{m_{v\perp}\, m_{v//}}} \; ; \quad m_v = \frac{eH}{m_{veff}} \; ;$$

$$\frac{1}{m_{veff}} = \frac{1}{\sqrt{m_{v\perp}\, m_{v//}}} \; ,$$

here m_e is the electron effective mass (nearly isotropic in our case) and $m_{v\perp}$ ($m_{v//}$) is the hole effective mass perpendicular (parallel) to the C-axis. From the slope of the N = 0 and N = even number transitions it is therefore possible to derive both the m_e and m_v effective masses ; whose values are reported in Fig. 8. A very good agreement with Thomas and Hopfield's values is obtained if the shoulder is associated to a $\Delta N = 4$ transition. We don't observe the $\Delta N = 2$ transition because it cannot be resolved from the stronger $\Delta N = 0$ line ; at our highest magnetic field another structure seems to be resolved on the Landau level and might be such a transition.

A similar analysis can also be performed for the structure at the B edge. Since in this case we observe only $\Delta N = 0$ transitions, from equation (5) we obtain:

$$\mu_B = (0.14 \pm 0.1)\, m_o \; .$$

The agreement with ref. (1) is good.

4.2. - E // C-axis.

In this case only the Γ_1 states are allowed. We don't observe any structure associated with A-edge since Γ_5 and Γ_6 are dipole forbidden. The structure at the B edges consist only of the Γ_1 component shifted to higher energy by 0.26 meV with respect to Γ_5. We notice the disappearence of the Γ_2 line described in the previous polarization. In principle we could have observed also the Γ_5 line because it is mixed to the Γ_1 by the magnetic field ; the separation

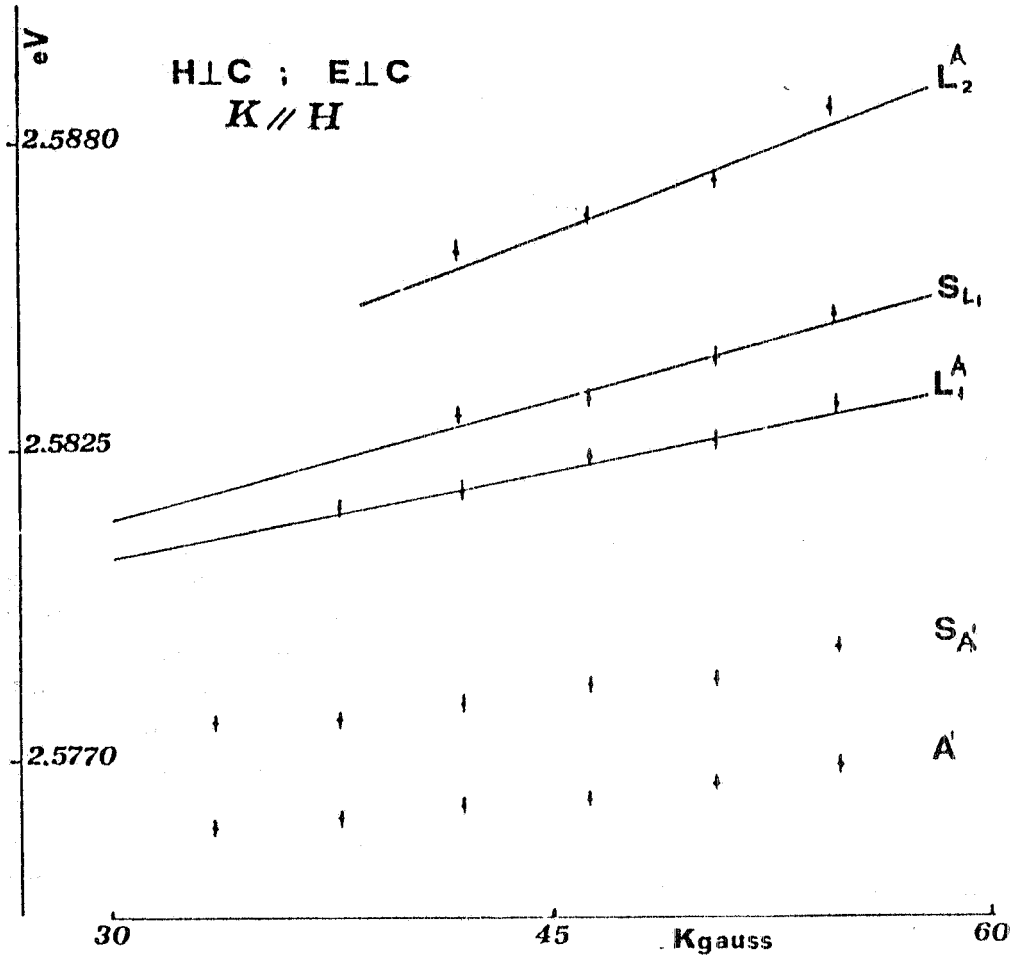

FIG. 8 - Energies with the A edge VS. magnetic field. From the slope of the L^A, L_2^A, S_L^A lines and from equation (5), assuming N = 4, we obtain:

$$\frac{\mu A}{m_o} = 0.16 \pm 0.01 \; ; \qquad \frac{m_e}{m_o} = 0.18 \pm 0.02 \; ;$$

$$\frac{m_{V_{eff}}}{m_o} = 1.7 \pm 0.1 \; .$$

The agreement with reference (11) is good.

from the Γ_1 however is too small to be observed in our experiment.

Similar measurements on CdSe are now progress. It is the first time that Landau levels in CdSe are detected; furthermore, forbidden excitons are observed. A detailed analysis on this sample will be reported as soon as possible.

ACKNOWLEDGEMENT. -

We are indebted to Prof. Franco Scaramuzzi for the use of the facilities at the cryogenic laboratory of the LNF.

REFERENCES. -

(1) - J. Barden, L. H. Hall and F. J. Blatt, in 'Photo conductivity Conference' (E. Brecknebridge, ed.) (Wiley, 1954), p. 146.
(2) - J. C. Phillips, J. Phys. Chem. Solids 12, 208 (1960).
(3) - L. M. Roth and B. Lax, Phys. Rev. Letters 5, 253 (1959).
(4) - G. F. Bassani and G. Pastori Parravicini, in 'Electron States and Optical Transitions in Solids' (Pergamon, 1975).
(5) - B. O. Seraphin and R. B. Hess, Phys. Rev. Letters 14, 138 (1965).
(6) - For an excellent review on modulation techniques see : M. Cardona, Modulation Spectroscopy, Solid State Phys. Suppl. 11 (1969).
(7) - R. L. Aggarwal, in 'Semiconductors and Semimetals' (R. K. Willardson and A. C. Beer, ed.) (Academic Press, 1972), v. 9.
(8) - R. L. Aggarwal and F. H. Pollak, Solid State Comm. 8, 1539 (1970)
(9) - CSCC/Cryogenics booklet, pag. 15.
(10) - G. Gatti, M. Iannuzzi, V. Montelatici, R. Bartiromo, E. Borsella and S. Mobilio, to appear in Solid State Communications.
(11) - J. J. Hopfield and D. G. Thomas, Phys. Rev. 122, 35 (1961); 116, 573 (1953).
(12) - R. G. Wheeler and J. O. Dimmock, Phys. Rev. 125, 1085 (1962).
(13) - J. Shah and T. C. Damen, Solid State Comm. 9, 1285 (1971).
(14) - F. Bassani and A. Baldareschi, Proc. Xth Intern. Conf. on Physics of Semiconductors, Cambridge (1970).
(15) - F. Bassani and A. Baldareschi, Proc. IXth Intern. Conf. on Physics of Semiconductors, Moscow (1968).